The mechanical and EM simulations of the CryoAC for the ATHENA X-IFU

D.Corsini[1,2 *], M. Biasotti[1,2], F. Gatti[1,2], M. De Gerone[1,2], C.Rossi[2], L. Piro[3], C. Macculi[3]
1 - University of Genova, Via Dodecaneso 33, 16146, Genova, Italy; 2 - INFN, Via Dodecaneso 33, 16146, Genova, Italy; 3 - INAF/IAPS, Via Fosso del Cavaliere 100, 00133, Roma, Italy

ABSTRACT

The design phase of the CryoAC for the ATHENA X-IFU has concerned numerical simulations to exploit different fabrication possibilities. The mechanical simulations have accounted for the peculiar detector structure: 4 silicon chips asymmetrically suspended by means of 4 microbridges each. A preliminary study was performed to analyze the response to acceleration spectra in the frequency domain, shocks and time domain random displacement, prior to a real vibration test campaign. EM simulations to spot unwanted magnetic fields have been conducted as well. In this work we will show the latest advance in the design of the new detectors, showing the main results coming from various simulations.

Keywords: CryoAC, ATHENA, X-IFU, simulations

1. INTRODUCTION

The need of an active Cryogenic Anticoincidence Detector (CryoAC) in the X-ray Integral Field Unig (X-IFU) of ATHENA has been already discussed (see for example ref. [1][2]). The CryoAC will be mounted in the X-IFU beneath the X-ray microcalorimeter chip at a distance of about 0.5mm to it to provide a veto signal when charged cosmic particles hit both detectors. It will work at the base temperature of 50-55mK with an energy threshold of 20keV, low enough to ensure an efficiency detection allowing the background reduction requirement of 0.005 cts/sec/cm^2/s/keV in 2-7keV TES array energy bandwidth. Our goal is the fabrication of a monolithic, silicon micromachined detector, from a 2 inches wafer, where four pixels are obtained with narrow slot cuts with deep etching of the silicon. The four pixels are suspended by means of 4 bridges each, and are arranged to form a hexagonal shape to fit the focal plane assembly (therefore each pixel comes out as a trapezoid). The design of this hexagonal shaped detector implies different type of simulations to make the best trade-off among detector operation requirements, its thermodynamic behaviour, and the overall robustness of the structure, which has to withstand different stresses during launches phases. Detector's requirements and detection principles are explained in other works of ATHENA CryoAC in these conference proceedings (see for reference papers no. 9905-88, 9905-185, 9905-187 in these proceedingss).

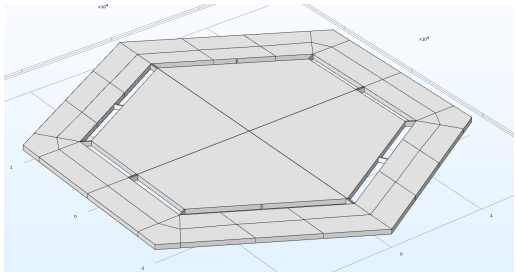

Figure 1. Drawing of the CryoAC detector in the COMSOL Multiphysics simulation toolkit. The outer part, called rim, will be connected to the focal plane assembly and act as thermal sink. Each of the four pixels are suspended by four bridges. An array of TES sensors covers the pixel surface in order to detect any kind of heat produced by particles passing through the silicon.

*Dario.corsini@ge.infn.it; tel. +39 010 353 6499

Space Telescopes and Instrumentation 2016: Ultraviolet to Gamma Ray, edited by Jan-Willem A. den Herder, Tadayuki Takahashi, Marshall Bautz, Proc. of SPIE Vol. 9905, 99055Y · © 2016 SPIE · CCC code: 0277-786X/16/$18 · doi: 10.1117/12.2232499

2. THE ATHENA DEMONSTRATION MODEL (DM)

While the design of the final CryoAC is getting to the final shape, some of the main aspects have yet to be confirmed.

In spite of the hexagonal shaped concept, the DM holds the previous design of a square chip, resembling one of the four foreseen for the total array. We are going to test this old design since we can have lots of informations, using this chip which will be easier to fabricate and test.

We found from simulations that, for our purposes, no important variations occur when considering a square chip instead of a trapezoidal one. Since the square chip is already under production, we decided to continue testing it, while simulations are now considering the new shape foreseen for the final array detector. That's why all simulations are conducted on a hexagonal overall geometry in the following.

The main features to be tested with the DM, and to be compared to simulations, are:

- Bridges manufacturing process;
- Anti-inductive wiring;
- Detection efficiency;
- Structure resilience (mechanical tests foreseen).

The results will help us to confirm our design or to address new features for the final detector array.

Figure 2 shows the overall design of the CryoAC DM.

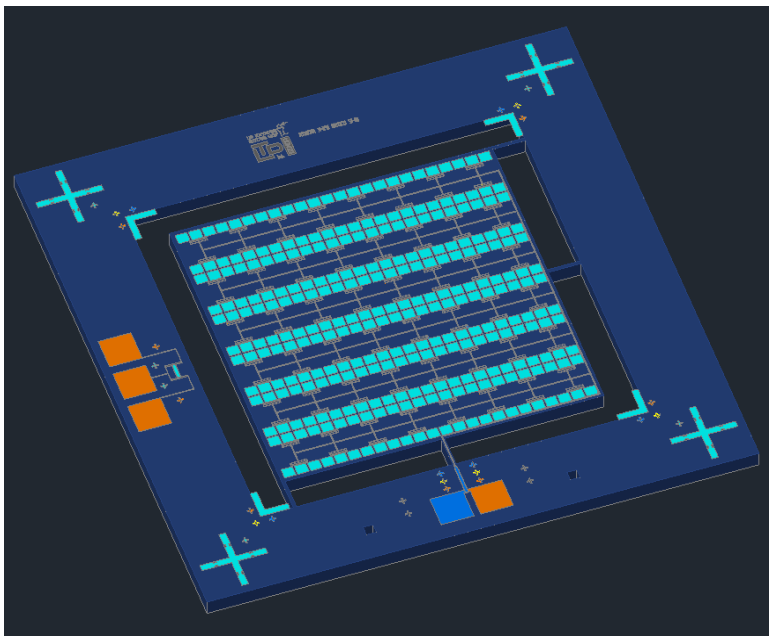

Figure 2. Design of the Demonstration Model (DM) for the CryoAC detector. It consists of a square Silicon pixel suspended by four bridges. For manufacturing reasons, it will be easier to produce and test this sample, giving us important feedbacks on the next stage detector, which will have the final, hexagonal shape.

While tests will refer to the above-discussed DM, in the following we will always refer to simulations conducted on the hexagonal shape.

3. THE ATHENA CRYOAC OVERALL DESIGN

The main parameters of the CryoAC are driven by Geant4 simulations of the cosmic background suppression index in the X-ray microcalorimeter array [2]. The required CryoAC detector thickness is 500µm and it must be placed 0.5mm beneath the microcalorimeter array. The total active area of the detector is also a requirement coming from simulations: the area results to be larger than that of the microcalorimeter array, to collect the slanted tracks. The hexagonal shape is due to the configuration of the focal plane. Since the array will fit this shape, the CryoAC has to be similar for fabrication and assembly purposes.

As it can be seen in Figure 1, the detector is composed of two main parts: the inner one is the particle sensitive area, while the outer one is the supporting frame and interface structure. The sensitive area is mainly composed by a silicon absorber which is covered by a uniformly distributed small TESs array. The quality of the calorimeter relies on the quality of the Silicon bulk crystal, of the materials deposited on it and on the manufacturing.

Due to the thermodynamics of the CryoAC, we know that it works at first order like a big calorimeter. The signal depends on two parameters: the total heat capacity of the detector and the heat conductance to the thermal bath [3]. First of all, since the detector is all micromachined, these two parameters are very well defined by the geometry. On the other hand, the heat capacity of the detector, i.e. the suspended silicon pixel, depends also on Silicon quality. The second parameter, the thermal conductance, can be controlled by means of the bridges size to the bath and their surface quality. The choice of the Silicon type for this kind of application is not an easy task: several Silicon wafers batches must be compared at 50mk.

The role of the bridges is first, for detection reasons, as they act as thermal link; second, they bear the active area of the detector avoiding breakages, and they must sustain stresses, which especially occur during the launch phases.

Being a fast rise time the main purpose of the CryoAC, in order to flag unwanted events, it might seems reasonable to adopt strong, solid (large) bridges. However, this configuration could lead to a strong thermal link and, so, to a fast thermal decay, meaning the detector has a short dead time (i.e. the shorter the duration of pulse, the lower the probability of having pile-ups). Unfortunately, being the rise time dependent on the quality of the Silicon crystal and on the conversion efficiency of the heat pulse by the sensors, the actual risk is to obtain a decay time equal or lower in respect to the rise time, which could lead to a suppression of the signal.

To make a summary of the detector configuration, Figure 3 shows a sketch of the main parts.

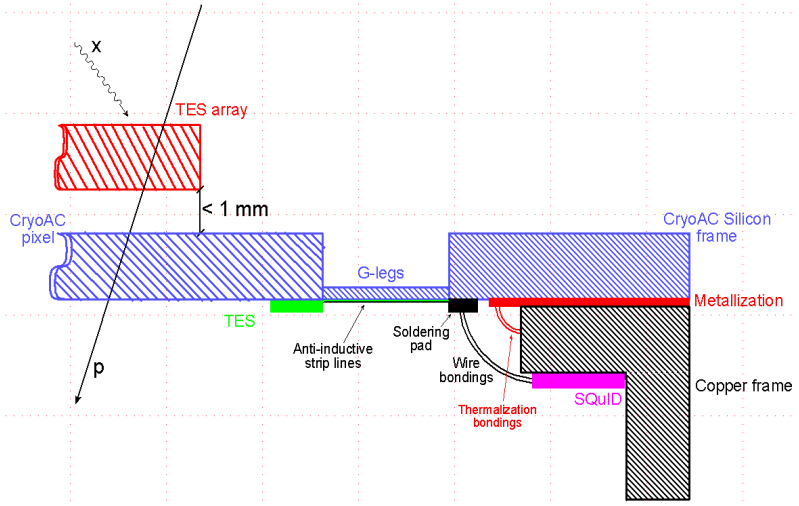

Figure 3. Sketch section of the array detector, together with the main TES X-ray array. G-legs, that is, silicon bridges, are drawn thinner just for understanding purposes. The 1mm distance is intended to be between the sensitive areas of both detectors (TES array and CryoAC).

4. SILICON BRIDGES DESIGN

Bridges connecting the detector to the external rim are placed on the two external sides of each pixel. No bridges are foreseen among pixels since we do not want thermal crosstalk effects. When designing these connections, we had to keep in mind both physics and fabrication processes. The role of the bridges is clear and crucial: they must fulfil these requirements:

- Withstand stresses applied to the detector during launch phases;
- Have the right thermal conductance at the operating temperature;
- They must host the path for electrical connections from the rim to the sensors.

The trade-off for the construction of the bridges came mainly from these three considerations.

Figure 4 shows some example of bridge geometries studied.

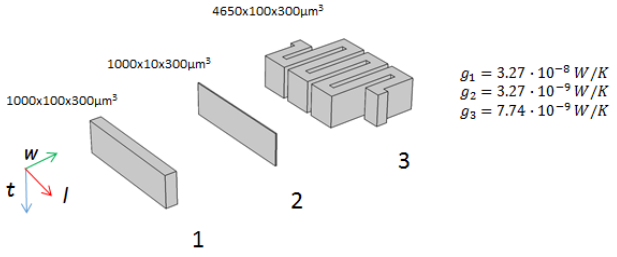

Figure 4. Some bridges used for simulations, with their respective thermal conductance calculated at 50mK

We used COMSOL Multiphysics and ANSYS tools in order to create a model for our detector. COMSOL has been used for raw mechanical analysis. Thermal and magnetic fields studies were then performed separately.

ANSYS was used to fully analyze the response to random vibration spectra.

In the following we will briefly describe the simulations carried out on our prototype design, and we conclude with some general remarks.

4.1 Thermal simulations

After defining the properties of silicon at low temperature, COMSOL Multiphysics software has been used to check the effective response of our chips to heat spots considering roughly the heat generated by a tens KeV source in hundreds of microns of silicon. This simulation is based on the assumption that a cosmic ray releases the kinetic energy of ten's KeV in a very small volume along the track in less than 1ps. Both heat capacity and thermal conductance are function of temperature, to account for small variations during the heating. For the heat capacity, we used the Debye Law, since T_{Debye} is 647.9K for Silicon, so a trend following $(T/T_{Debye})^3$. For the thermal conductance, we extrapolated it down to the working temperature starting from the work of Sota et al. [4].

Figure 5 shows the thermalization response in the bulk of the pixel.

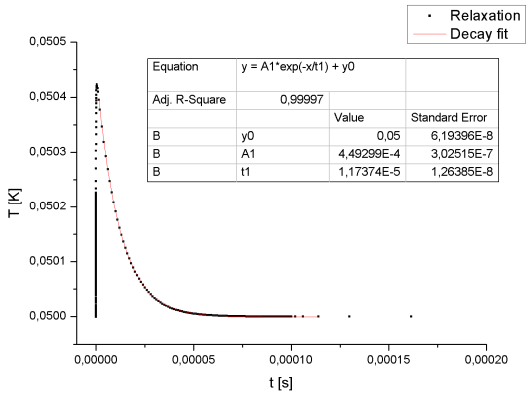

Figure 5. Reconstruction of a thermal pulse event. The fit is useful to understand the relaxation time.

4.2 Mechanical simulations

For flight qualification, many parameters have to be taken into account.

While bridges must be designed for good thermal properties, they also have to fulfil strict mechanical requirements. We checked with COMSOL and ANSYS simulations different aspects of the detector from the mechanical point of view:

- Body load, plus an acceleration force up to 2000 times g;
- Search for main eigenfrequencies, and a modal analysis to check for detector behaviour;
- Random vibration analysis for a given Amplitude Spectral Density (ASD)

In all these simulations we had to consider three main constrains: 1) the detector has to stay at least an order of magnitude below the breaking point of crystalline Silicon [5]; 2) during random vibrations or acceleration displacement, it must not hit the above Silicon wafer which hosts the X-ray detector, 500µm distant; 3) its natural frequencies have to be far from the resonances at which the focal plane will be stressed during launch phases.

An important thing to be kept in mind is that simulations results may vary strongly depending on fixing parameter. In our simulations, we fixed a section of the external part of the rim, giving rise to an infinite stiffness in that section (see Figure 6). This, of course, does not depict a real situation, where the detector will be anchored to the focal plane with a lot of different features, nor it consider how the focal plane is fixed, piece by piece, to the rocket. We are aware that, while some simulations give us confidence on their results, some other will need adjustments, as new details will be given until the final assembly is known.

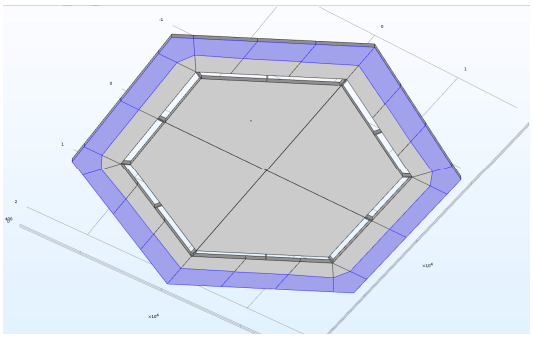

Figure 6. The blue area shows the fixed part of the detector.

In Figure 7 and 8 we show the maximum displacement result for a continuous acceleration up to 2000 g, probed at the outermost tips of the Silicon chips, and the stress profile for each of the 4 bridges of one of the pixels (We considered only a set of bridges due to axial symmetry). As it can be seen, in both cases we are well under safety levels both for sweep distance and for stress level on bridges, being the yield strength of Silicon 7GPa.

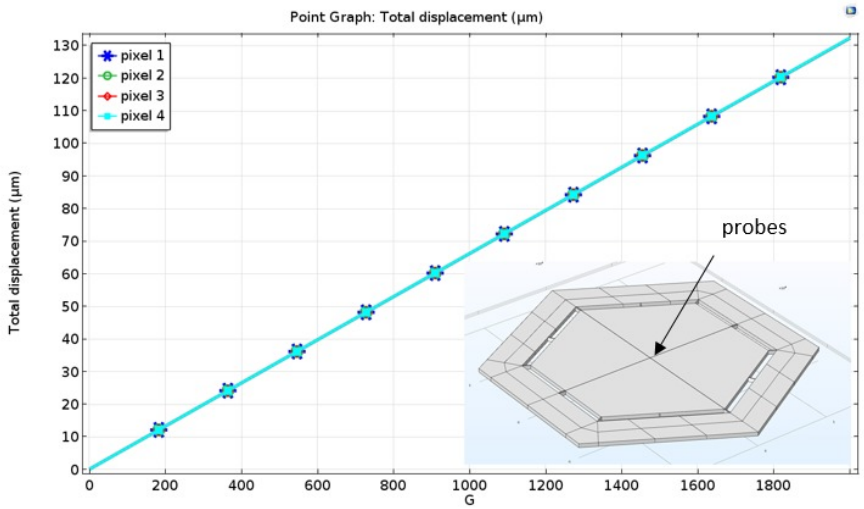

Figure 7. Displacement profile of the outermost tips of the floating chips

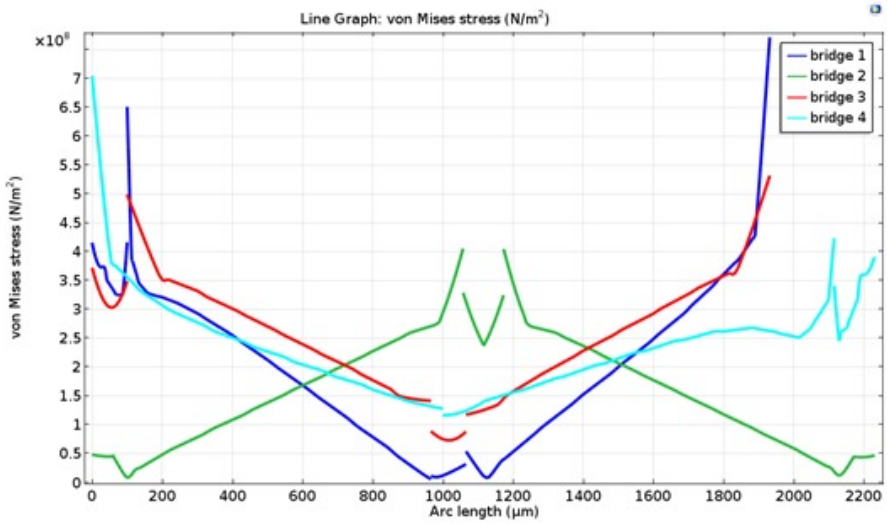

Figure 8. Stress profile along the length of the 4 bridges of one pixel, taken at 2000G

Concerning the modal analysis, a combined study with COMSOL and ANSYS for a comparative analysis has been done, with consistent results. Below we show the resulting spectra over 35kHz. Main frequencies are spotted above 2.5kHz, and this is encouraging, since we know we have to avoid low frequencies, up to 2kHz (see Figure 10 below for reference).

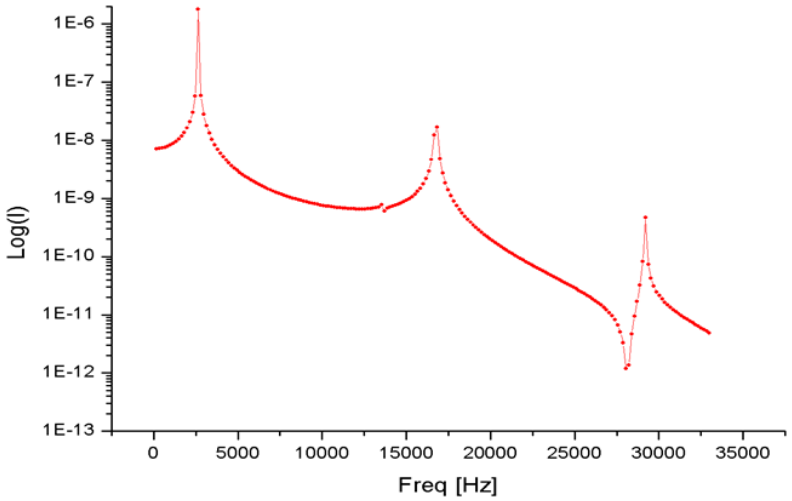

Figure 9. Modal analysis of our prototype detector with peaks at main frequencies.

As a result from the Power Spectra Analysis, we obtained, using ANSYS software, good results. Giving as input the spectra in Figure 10, we simulated the response to a random vibration test, which, of course, will be verified with a campaign of testing of prototype chips, under construction.

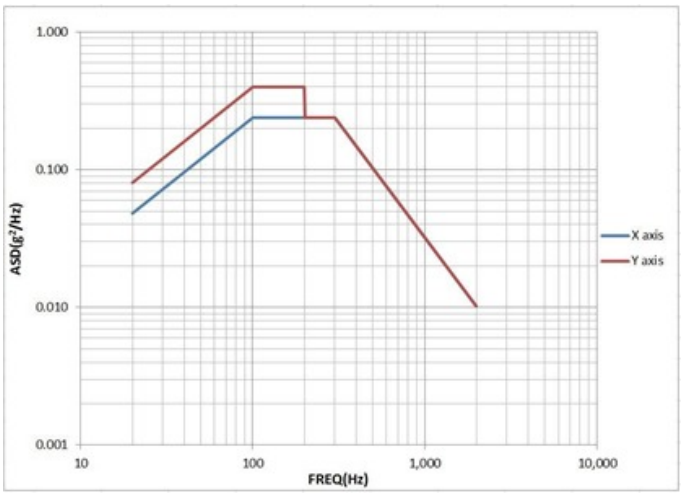

Figure 10. Reference spectra used for our analysis.

The ANSYS 15.0 simulations highlight a maximum equivalent stress of 6MPa and a maximum displacement of 1.92 microns, relative to the base of the structure (i.e. the fixed supports). The results are scaled by two times to get the two sigma values equivalent to a 95.45% probability. However it should be noted that the directional results are statistical quantities and cannot be combined or transformed in any vectorial sense. A meaningful value of the equivalent stress is computed with a special algorithm by Segalman-Fulcher [6].

Resulting responses are shown in following Figure 11 and Figure 12. Plots show the maximum displacement is about 2μm, while the stresses on bridge does not even reach 10MPa. These results show our geometry is well below the critical values and also that we have room for some requirement relaxations in the design of our chip.

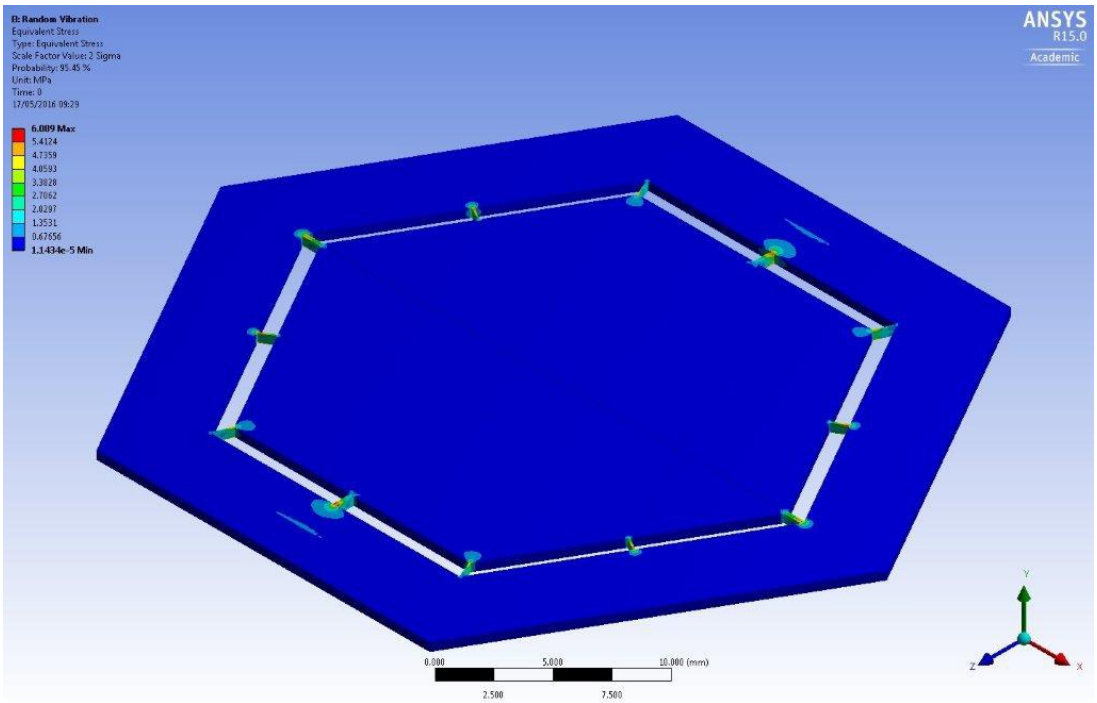

Figure 11. Random vibration analysis: stress.

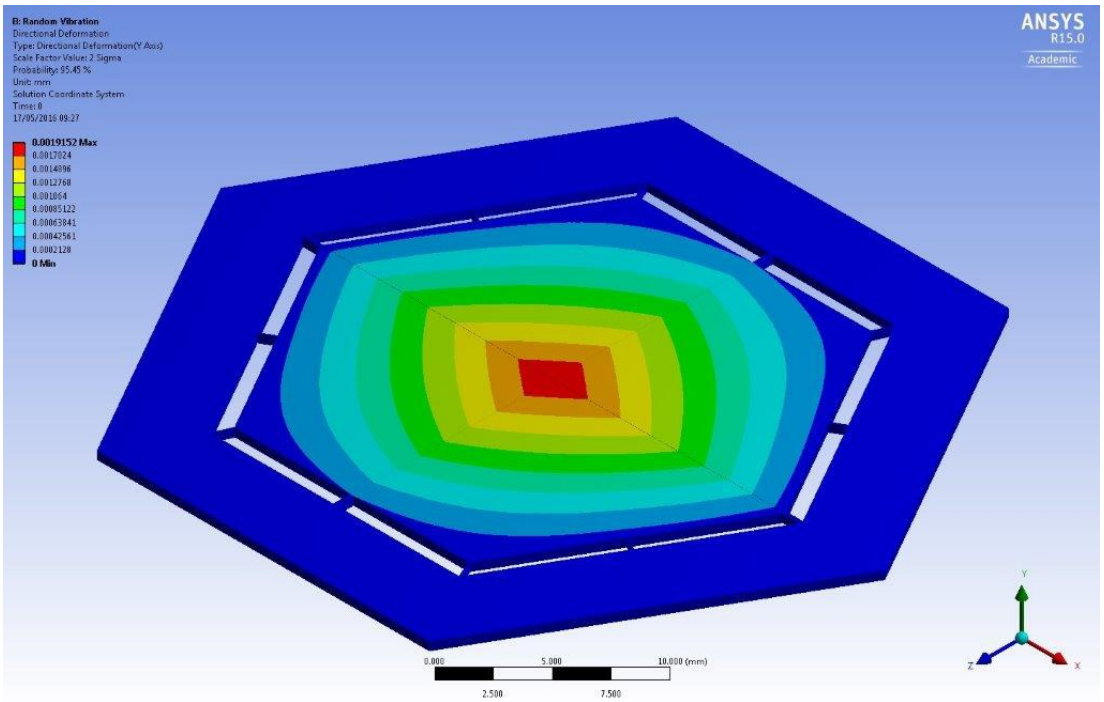

Figure 12. Random vibration analysis: displacement.

4.3 E.M. simulations: single pixel

The last topic we have to focus on is that of magnetic interferences of our detector on the above X-ray TES microcalorimeter array.

Since the CryoAC detector will be read out in DC mode, no risk of inductive or capacitive coupling at high frequency is present. On the other hand, the X-ray TES array will work in AC multiplexing regime, and possible back crosstalk to the CryoAC must be carefully checked. Since TESs have shown a weak link effect with diffractive pattern of the gain versus the magnetic field intensity, we have done an extensive work to minimize the DC magnetic field of the bias currents. The first thing we did in designing our device was to include anti-inductive stripline wiring, in order to suppress any sort of loops. Of course, as shown in Figure 13, it was not possible to avoid small loops at every TES end.

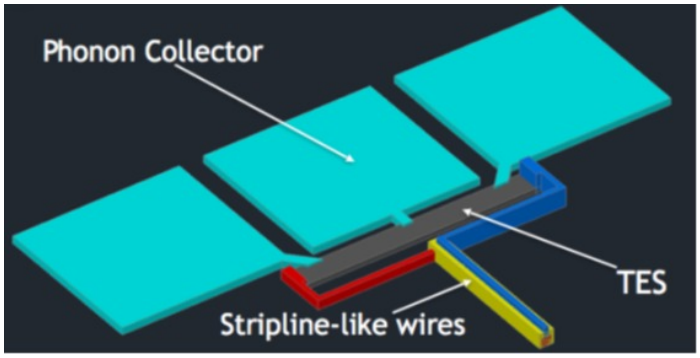

Figure 13. Detail of one single TES detector, showing a small loop is present at every TES. Normal DC biasing will not cause any interference along the stripline wiring, but loops at TES level could, in principle, create magnetic field up to the main array detector.

Figure 14 shows the COMSOL model used for this study.

To be sure no disturbances will get to the above detector, we simulated a DC bias current along the small part related to the TES only, and found encouraging results, since the expected magnetic field, which should be below the safety level of 1μT at X-ray TES array, is well below 2-3 order of magnitudes that level, as can be seen in Figure 15. Work is already on going with the SRON team to optimize the CryoAC TES configuration.

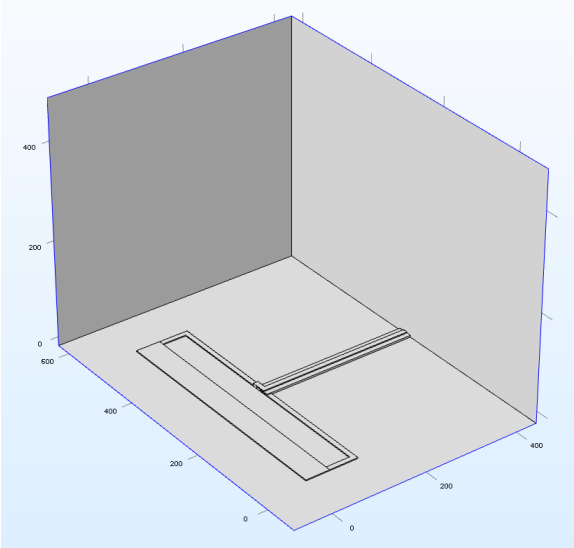

Figure 14. COMSOL model for the study. A constant bias current was assumed.

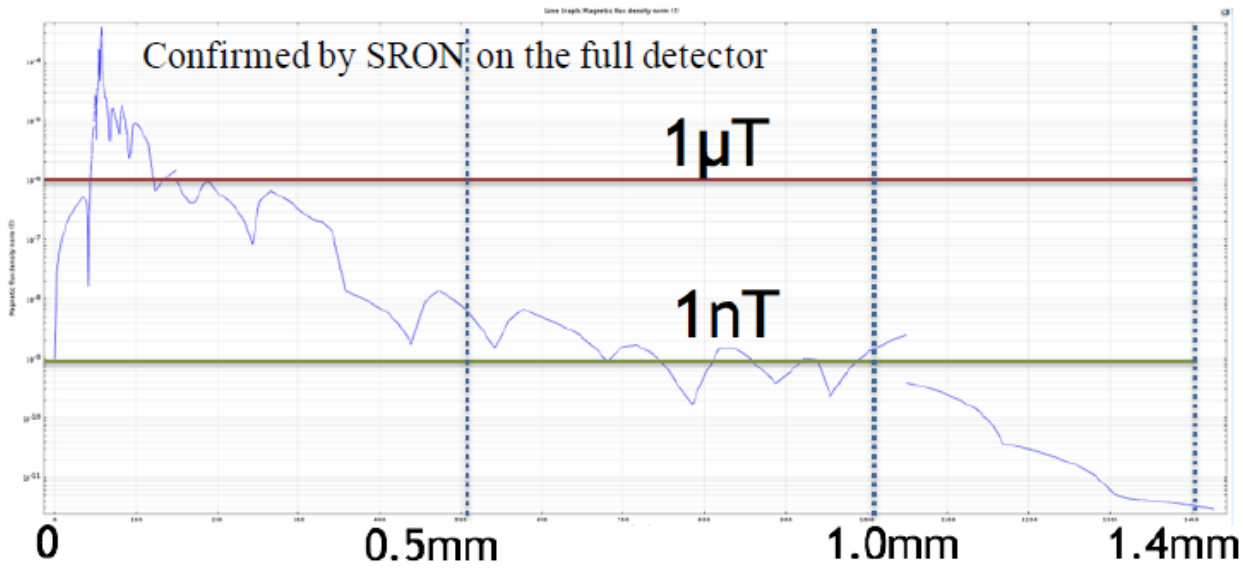

Figure 15. Result of the simulation. The x axis represent the vertical distance between the CryoAC surface and the main array, showing any fields drop fast under 1nT before reaching the active part of the X-ray detector.

5. CONCLUSIONS

In order to manufacture the future cryogenic anticoincidence detector for the mission ATHENA, a lot of efforts have been put to identify the most functional set up.

Along with the developing of a fast flag detector for anticoincidence signal, the need to develop a space qualified object lead us to push continuously with simulations for mechanical, thermal and electrical behaviors.

Although some good parameters have been found, we are working on it to increase the readiness level of this device and to obtain the best detector for the purpose.

In few months, fabrication and test (mechanical and functional) of the device will start, allowing us to check if our simulations were correct, and were to focus to improve our object.

Work is on going with the SRON team to optimize the CryoAC TES configuration in order to produce very low effects on the TES array.

6. ACKNOWLEDGEMENTS

This work has been partially supported by ASI (Italian Space Agency) through the Contract no. 2015-046-R.0, and by ESA (European Space Agency) through the Contract no. 4000114932/15/NL/BW

We thank Dr. Henk Van Weers, SRON (the Netherlands) for the support given in setting up the random displacement simulation, and for fruitful discussions.

REFERENCES

[1] C. Macculi et al., “The Cryogenic Anticoincidence Detector for ATHENA-XMS”, Journal of Low Temperature Physics 167, 783–794 (2012).

[2] S. Lotti et al., “Background simulations for the ATHENA X-IFU instrument: impact on the instrumental design”, Proc. SPIE 9144, 91442O, (2014).

[3] K. D. Irwin e G. C. Hilton, “Transition-Edge Sensors” in Cryogenic Particle Detection, April 29, 2005.

[4] T. Sota, K. Suzuki, D. Fortier, "Low-temperature thermal conductivity of heavily doped p-type semiconductors", J. Phys. C: Solid State Phys. 17 (1984) 5935-5944.

[5] Kurt E. Petersen, “Silicon as a Mechanical Material" Proceedings of the IEEE, vol. 70, no. 5, May 1982.

[6] Segalman-Fulcher, “An efficient method for calculating rms Von Mises stress in a random vibration environment”, Journal of Sound and Vibration 230.2 (2000): 393-410.